Modeling Dielectric Absorption in Capacitors

Ken Kundert
Designer's Guide Consulting, Inc.

Version 2e, August 2021

It is well known that dielectric absorption plays a critical role in determining the accuracy of analog sampled-data systems that are based on charge storage, such as sample-and-holds and switched-capacitor ADCs. Less appreciated, but no less important, is the role it plays in determining the quality factor, or *Q*, of the capacitor. Dielectric absorption has both storage and loss components that act, and are significant, over the entire usable frequency range of the capacitor.

Along with background information on the origins of dielectric absorption, this paper presents two models for a capacitor that exhibits dielectric absorption. The first is the relatively well known model proposed by Dow. The second is a model with relatively little exposure that is based on the dielectric permittivity model of Cole and Cole. This model has fewer parameters than the Dow model and is predictive over a very broad range of frequencies.

This manuscript was originally written in March 1982 and was revised in October 2001. It was last updated on August 18, 2021. You can find the most recent version at www.designers-guide.org. Contact the author via e-mail at ken@designers-guide.com.

1.0 Introduction

A fundamental limitation in the accuracy of sample-and-holds and A-D converters is a phenomenon called dielectric absorption, which also goes by the names of dielectric relaxation and soakage [20]. Dielectric absorption is the tendency of a capacitor to recharge itself after being discharged. While not widely appreciated, dielectric absorption is also the dominant loss model over the entire usable range of most capacitors, and so can also affect the performance of high-Q circuits such as VCOs.

This paper covers the symptoms of dielectric absorption in both the time and the frequency domains, the physical mechanism that causes it, and the process of modeling it.

2.0 Symptoms

If a capacitor remains charged for a long period of time and then is briefly shorted, the voltage on the capacitor will slowly tend to recover to a fixed percentage (typically between 0.01% and 10%) of its original value. This percentage is a simple measure of dielectric absorption. The amount of dielectric absorption a capacitor exhibits is highly dependent on the dielectric material: polystyrene, polypropylene, and teflon display very little absorption, while ceramic is a much poorer performer. SiO_2 displays about 0.1% dielectric absorption, putting its performance in the middle of the pack [12,16]. Recovery that results from dielectric absorption can be simply modeled with the circuit in Figure 1.

FIGURE 1. *A simple model for an absorptive capacitor and its response to a negative current impulse.*

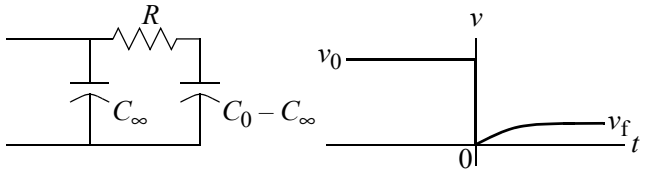

This simple model is a good first step, but it is unable to properly model the time constant of the recovery, or relaxation, period for most dielectrics. After releasing the short on the capacitor, the voltage will initially build back very quickly. In usually 1 to 10 seconds, 50% of the final value is reached. But then the recovery process slows considerably and it often takes 20 minutes to close within 5% of the final value. This means that many more time constants will be required to properly model dielectric absorption.

The model of Figure 1, though an over simplification, shows the dielectric absorption has aspects of both memory and dissipation. The memory is provided by the supplemental capacitor C_0–C_∞, making the effective capacitance larger at low frequencies than at high. The dissipation is provided by the resistor R. It is the loss provided by R that makes dielectric absorption of interest to designers of high-Q circuits. It is the wide range of time constants of dielectric absorption, not modeled in Figure 1, that causes both the memory and the dissipation aspects to be noticeable over the capacitor's entire usable frequency range.

Shown in Figure 2 is a plot of both the resistive and reactive parts of the impedance of a 10 nF X7R[1] multilayer monolithic ceramic capacitor. Notice the behavior of the resistive portion of the impedance. It has roughly a one pole slope from 10 kHz to 10 MHz, where it flattens out and then turns up again. This behavior has been widely observed [18,23]. At high frequencies, the resistance is dominated by loss in the conductor (the leads and the plates). It increases roughly in proportion to $\sqrt{f}$ at high frequencies due to skin effect. At low frequencies, the resistance is dominated by losses in the dielectric: dielectric absorption. It decreases roughly in proportion to f^{-1}. This is consistent with the empirical observation that the dissipation factor (tan δ_D) for many capacitors is almost constant in their usable frequency range [23]. Resistance is related to dissipation factor by

$$R = \frac{\tan\delta_D}{C\omega} \tag{1}$$

FIGURE 2. *Resistance (R) and reactance (X) of a 10 nF ceramic capacitor.*

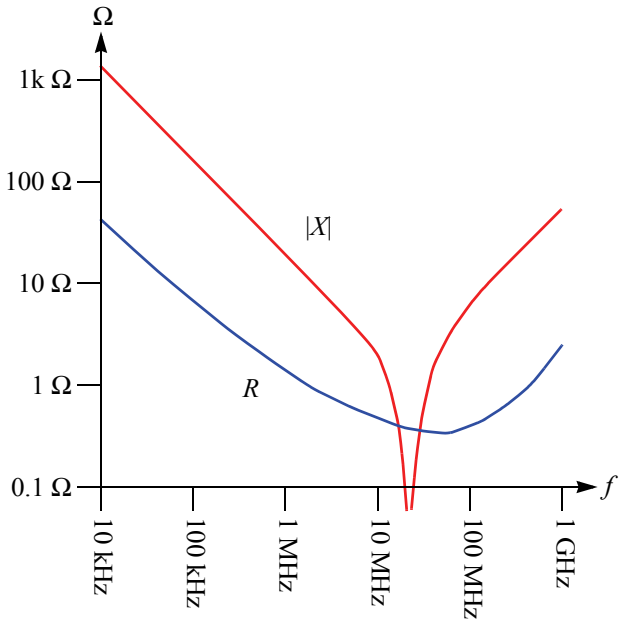

3.0 Polar Dielectrics

The permittivity of a dielectric varies with frequency as various mechanisms within the dielectric are excited [5]. As an electric field impinges on a dielectric material, the charge particles in that material will rearrange themselves in such a way as to line their dipole moments up with the field. This acts to increase the flux density and therefore the permittivity. This is shown for a polar material in Figure 3. Region (1) is in the range of

1. The X7R designation indicates that the capacitance deviates no more than ±15% from nominal over the –55 C to 125 C temperature range.

X-rays and above. At these frequencies there is no interaction between the material and the wave, and so the permittivity (ε) is the same as the free space permittivity (ε_0). As frequency decreases the inner electrons (2), the valence electrons (3), and eventually the atoms (4) themselves successively resonate and make their contributions to the permittivity. Notice that during these resonances the permittivity becomes complex ($\varepsilon = \varepsilon' + j\varepsilon''$), which indicates that the dielectric becomes lossy. As frequency descends, polar molecules (5), or in some materials, electric domains, become excited and increase the permittivity greatly. For the polar molecules this is called dipole relaxation, while for the electric domains it is called ferroelectric relaxation (so named because of its similarity to ferromagnetism) [4, 21]. These two represent the mechanism behind dielectric absorption. The last process that affects permittivity is called space charge relaxation (6). This is caused by charges that are free to move about but not to recombine at the electrodes. These charges behave at low frequencies like macroscopic dipoles that reverse their direction each half period.

FIGURE 3. *Permittivity characteristics of a polar dielectric versus frequency.*

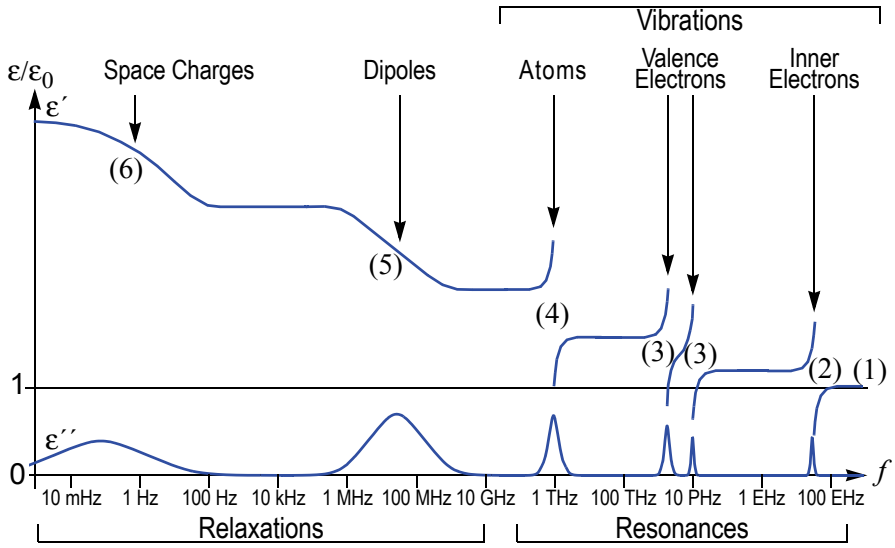

DeBye first showed that for polar molecules in gaseous form the permittivity versus frequency could be written as follows [9]:

$$\varepsilon(\omega) = \varepsilon_\infty + \frac{\varepsilon_0 - \varepsilon_\infty}{1 + j\omega\tau} \tag{2}$$

where ε(ω) is the complex permittivity ($\varepsilon = \varepsilon' + j\varepsilon''$), ε_∞ is the permittivity at frequencies above dipole relaxation, ε_0 is the permittivity at frequencies below dipole relaxation, and τ is the relaxation time constant. This behavior is accurately represented by the model of Figure 1.

It was later shown by Cole and Cole that this equation does not adequately predict the behavior of liquid and solid dielectrics [6]. They measured a large number of materials and found that when ε′′ was plotted versus ε′, a curved arc resulted, whereas a semicir-

cle was predicted by the DeBye relation. They were able to modify the DeBye relation in order to fit the new data for non-gaseous dielectrics. The Cole and Cole relationship is:

$$\varepsilon(\omega) = \varepsilon_\infty + \frac{\varepsilon_0 - \varepsilon_\infty}{1 + (j\omega\tau_0)^{1-\alpha}} \text{ where } 0 \le \alpha \le 1 \quad (3)$$

This equation models the ε′-ε′′ curve as a portion of a circle with its center below the ε′ axis. The constant α is a measure of how far the center is below the axis. In Figure 4 the effect of α on both ε′′ versus ε′ and the impedance of an otherwise ideal capacitor is shown. Note that at $1/\tau_0$ both the asymptotic slopes of the resistance and the effective capacitance changes, and the width of the transition is very sharp for the DeBye dielectric (α = 0) and becomes very wide as α increases.

Given the Cole and Cole relationship:

$$Z(\omega) = \left[j\omega \left(C_\infty + \frac{C_0 - C_\infty}{1 + (j\omega\tau_0)^{1-\alpha}} \right) \right]^{-1} \quad (4)$$

where $Z(\omega)$ is the impedance of the capacitor, $C_\infty = A\varepsilon_\infty/d$ is the high frequency capacitance, $C_0 = A\varepsilon_0/d$ is low frequency capacitance, A is the area of the parallel plate capacitor, and d is the distance between the plates.

Notice that as ω goes to zero the slope of the resistance on a log-log plot approaches –α. As ω goes to infinity the slope of the resistance on a log-log plot approaches –(2–α). And finally, when α = 0, the Cole-Cole relation is identical to DeBye's.

It can be shown that the Cole-Cole relation is made up of an infinite number of DeBye relaxation processes. In a gas where the molecules are relatively simple and independent, a single time constant dominates. In a liquid or a solid, the molecules can be very large or be bound in a lattice. This makes the reorientation of polar molecules subjected to an electric field a slow and complicated process. In addition, some polarization of the dielectric may be due to physical charges accumulating on grain boundaries of polycrystaline materials, charges tunneling to the surface states at the plate interface, or the formation of electric domains. The time constants associated with these dipoles may range from nanoseconds to minutes or longer [12].

Since dipole relaxation is a molecular process, it shows anisotropic properties as well as temperature dependence. Ferroelectric relaxation also shows a temperature dependence up to its Curie temperature, when the electric domains break down and the effect disappears just as in ferromagnetic materials. Absorption in dielectrics is also a strong function of the amount and type of impurities in the dielectrics. Water in printed circuit laminates is responsible for a form of dielectric absorption called "hook" that causes many problems for users of high impedance and high frequency attenuators.

For some materials the ε′-ε′′ diagram is not symmetric, as shown in Figure 5. This can be reasonable well modeled by a formula proposed by Davidson and Cole [8]:

$$\varepsilon(s) = \varepsilon_\infty + \frac{\varepsilon_0 - \varepsilon_\infty}{(1 + s\tau_0)^\alpha} \quad (5)$$

FIGURE 4. *Dielectric Cole-Cole and impedance plots for various values of* α.

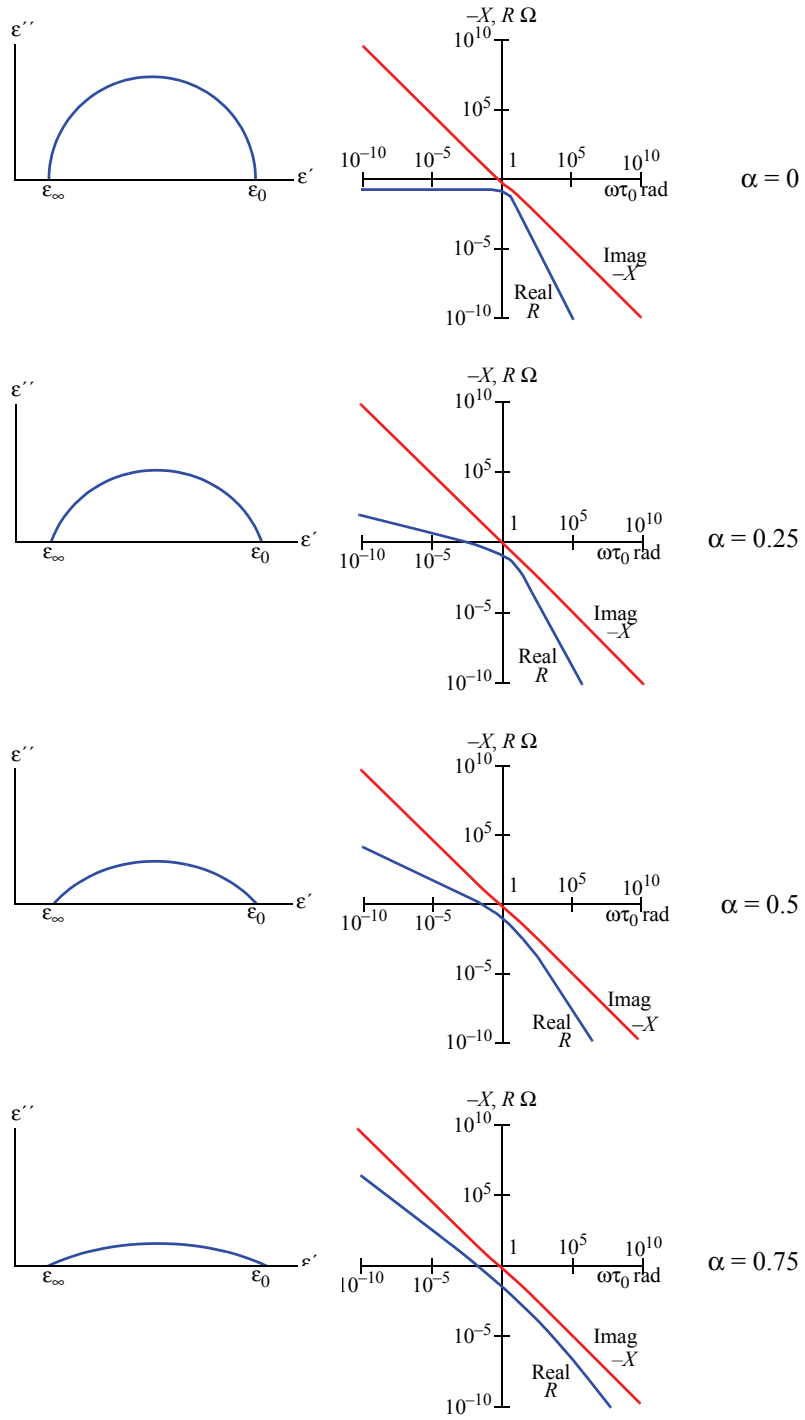

for $0 \le \alpha \le 1$. This model does not seem to apply for most capacitors and so will not be considered further.

FIGURE 5. *Skewed Cole-Cole diagram.*

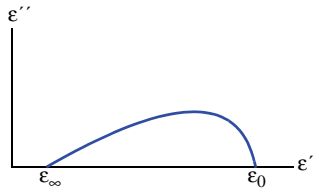

4.0 Modeling Absorptive Capacitors

Dielectric absorption in a capacitor is difficult to characterize accurately because of the very wide range of the time constants involved and because of the high level of performance required in the measuring equipment. To get a good characterization, the capacitor response must be measured for a range of frequencies at least three decades higher and lower than $1/\tau_0$. Frequency domain measurements must be made with vector impedance analyzers that can accurately resolve a small resistive component in a largely reactive impedance (they must be able to accurately measure large values of Q). In the frequency domain the resistive portion of the impedance gives the most information about dielectric absorption. In the time domain, which is usually used for measurement longer than 100 ms, an ammeter is needed with very low bias current and the ability to resolve very low currents. If these instruments are available, then an accurate and complete model can be made, but such a model is often not required. To completely model dielectric absorption would require, in most cases, a range of accuracy that spans ten decades of frequency or more. Generally, however, the application does not warrant such a model and one can get by with a model that is faithful to the behavior of the physical component over a much smaller range of frequencies.

There are two different approaches to making the measurements in the time domain needed to characterize dielectric absorption. In the ‘discharge current’ approach, the capacitor is charged for a very long time and then abruptly shorted, and the current that passes through the capacitor is measured versus time. This is the preferred approach. The second approach is referred to as the ‘voltage recovery’ approach. Here, the capacitor is again charged for a long time and abruptly shorted, but the short is quickly removed and the voltage on the capacitor is measured versus time. There are several substantial errors present in this method that act to limit the achievable accuracy. The most important involves how long the short is maintained. Conceptually, the short should drain the charge in C_∞, but not drain any charge that has been absorbed by the dielectric. Thus, the short should create a current impulse, and so should have infinitely short duration, which of course is not practical. Consider, if this test were made by shorting out a charge capacitor for 1 ms. All the energy stored in dielectric absorption time constants of less than 1 ms would be lost. Consequently, the recovery voltage would be significantly lower than if a true current impulse were used. Another problem with this method is that since a voltage is present on the capacitor, there is more error

due to leakage resistances and bias currents. In addition, more resolution is needed from the measuring equipment than with the discharge current method.

Two approaches for generating a model are presented, one from time-domain data that was first proposed by Dow, and one from frequency-domain data that is based on the Cole-Cole parameters. Also presented are insights into how to derive the Cole-Cole parameters from both time-domain and frequency-domain data. I will only briefly cover the time-domain method as it is relatively well known. The Cole-Cole parameters method will be given a more complete coverage since it has had considerably less exposure in the circuit design community.

4.1 Dow Method

For the time-domain modeling method presented by Dow, the absorptive capacitor is charged for a long time and suddenly shorted. The discharge current is carefully measured and plotted [11,14]. This is done in Figure 6 for a 1 µF polystyrene capacitor.

FIGURE 6. *Absorptive capacitor discharge current.*

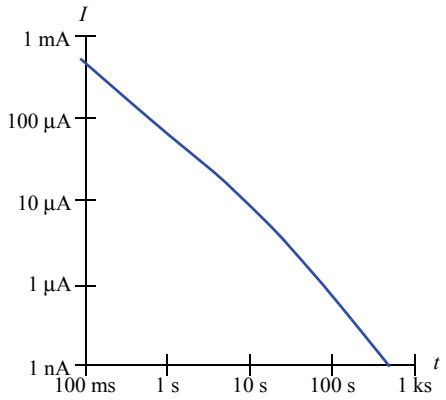

This voltage step response can be approximated by a summation of decaying exponentials,

$$\frac{I}{V_0} = C_\infty \sum_k a_k e^{-t/\tau_k} \tag{6}$$

Since there is no ringing in the step response the exponentials are real and can be modeled as RC pairs. We are summing currents into a short circuit and therefore the RC pairs will be added in parallel to C_∞. A sixth-order model is shown in Figure 7 with the time constants to fit the data in Figure 6 given in Table 1. The values are computed with

$$C_\infty = 1\ \mu\text{F} \tag{7}$$

$$R_k = \frac{1}{a_k C_\infty} \tag{8}$$

FIGURE 7. *Absorptive model of a 1 μF polystyrene capacitor, values are given in Table 1.*

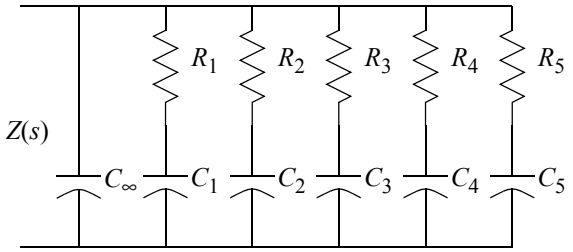

TABLE 1. *Data for the model of Figure 7.*

k	R_k	C_k	C_k/C_∞	R_kC_∞	$\tau_k=R_kC_k$
1	3600 GΩ	140 pF	1.4×10^{-4}	3.6×10^{6}	500
2	250 GΩ	200 pF	2.0×10^{-4}	2.5×10^{6}	50
3	20 GΩ	270 pF	2.7×10^{-4}	2.0×10^{6}	5.4
4	3 GΩ	190 pF	1.9×10^{-4}	3.0×10^{6}	0.58
5	330 MΩ	120 pF	1.2×10^{-4}	3.3×10^{6}	0.04

$$C_k = \frac{\tau_k}{R_k} \tag{9}$$

4.2 Cole-Cole Parameter Method

Cole and Cole developed a model with only four parameters that is more predictive that the one developed by Dow. They showed that it was possible to model a capacitor with an absorptive dielectric as shown in Figure 8 [6].

FIGURE 8. *Cole-Cole model for an absorptive capacitor.*

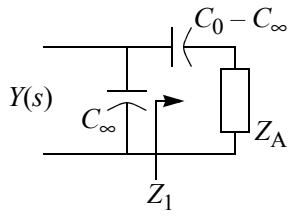

Z_A is found by removing C_∞ and $C_0 - C_\infty$ from the expression for $Y(s)$.

$$Y(s) = sC_\infty + \frac{(C_0 - C_\infty)s}{1 + (s\tau_0)^{1-\alpha}} = sC_\infty + Y_1(s) \tag{10}$$

$$Y_1(s) = \frac{(C_0 - C_\infty)s}{1 + (s\tau_0)^{1-\alpha}} = \frac{(C_0 - C_\infty)s}{1 + \frac{s\tau_0}{(s\tau_0)^{\alpha}}} = \frac{1}{Z_1(s)} \tag{11}$$

$$Z_1(s) = \frac{(s\tau_0)^{\alpha} + s\tau_0}{(C_0 - C_\infty)(s\tau_0)^{\alpha} s} \tag{12}$$

$$Z_1(s) = \frac{1}{(C_0 - C_\infty)s} + \frac{\tau_0}{(C_0 - C_\infty)(s\tau_0)^{\alpha}} \tag{13}$$

$$Z_1(s) = \frac{1}{(C_0 - C_\infty)s} + Z_A(s) \tag{14}$$

$$Z_A(s) = \frac{\tau_0}{(C_0 - C_\infty)(s\tau_0)^{\alpha}} \tag{15}$$

Z_A has some interesting properties that make it a particularly easy function for which to synthesize an approximation. Notice that Z_A is proportional to $s^{-\alpha}$, so its Bode plot is simply a straight line with a slope of $-\alpha$. Notice also that the ratio of X_A/R_A is constant over frequency and consequently so is the phase of Z_A, which equals $-\pi\alpha$. An exact model of Z_A would be distributed, but a lumped approximation is created simply by alternating poles and zeros exponentially along the real frequency axis, as shown in Figure 9.

FIGURE 9. *A lumped approximation to Z_A.*

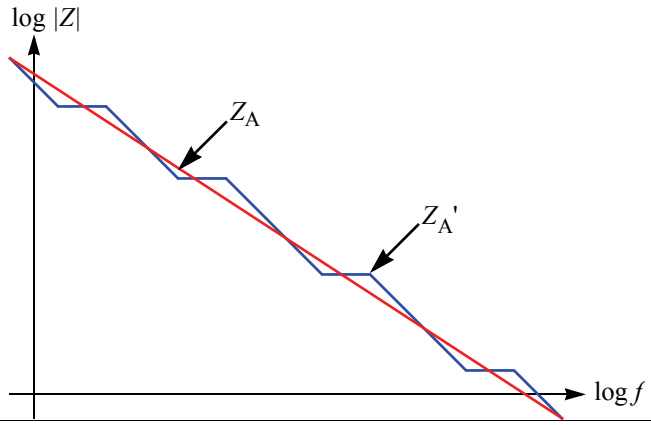

Once the frequency range of interest is chosen, the accuracy is solely dependent on the order of the approximation network, while the slope of the approximation in the range of interest is controlled by the relative spacing between the poles and zeros.

This model is easily generated once the Cole-Cole equation parameters are known. These parameters are related to features of both the time- and frequency-domain responses in the following paragraphs to aid in the process of their discovery.

Cole and Cole showed that the discharge current of a capacitor that has been charged for a long time and suddenly shorted follows the curve shown in Figure 10 [7]. For values of time much greater than τ_0 the current asymptotically approaches a slope on a log-log scale of $-(2-\alpha)$. For values of time much less than τ_0 the slope approaches $-\alpha$ (one can also see these slopes in the measured data of Figure 6).

FIGURE 10. *Absorptive capacitor discharge current.*

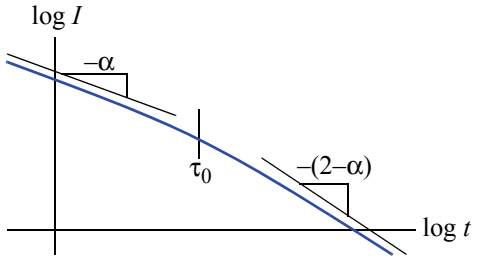

The following observations stem from the frequency domain plots of Figures 4:

1. The capacitance equals C_∞ for $\omega \gg 1/\tau_0$.
2. The capacitance equals C_0 for $\omega \ll 1/\tau_0$.
3. C_0 is always greater than C_∞.
4. $1/\tau_0$ is near the frequency where the ratio of X/R is the smallest[2].
5. The log-log slope of R at $\omega \ll 1/\tau_0$ is $-\alpha$.
6. The log-log slope of R at $\omega \gg 1/\tau_0$ is $-(2-\alpha)$.
7. As α increases, so does the ratio of X/R at $\omega = 1/\tau_0$.
8. As C_0 approaches C_∞, R decreases.

Given the above information, the right equipment, and enough patience, it should be possible to determine C_0, C_∞, α and τ_0. This was done for the capacitor characterized in Figure 2. Using only the information contained in Figure 2, the following Cole-Cole parameters were chosen:

$C_\infty = 10$ nF
$C_0 = 22.5$ nF
$\tau_0 = 1$ s
$\alpha = 0.75$

From this data, Z_A calculated using (15) and plotted in Figure 11, is

$$Z_A = \frac{1}{(12.5\text{ nF})s^{0.75}} \tag{16}$$

Also plotted in Figure 11 is Z_A', the lumped approximation to Z_A. Notice that the first critical frequency is a pole. This results in Z_A being finite at DC, which gives a DC

2. For $\alpha = 0$, $1/\tau_0$ and this frequency are identical, but as α increases this frequency increases to a value above $1/\tau_0$.

FIGURE 11. *Bode plot of Z_A and Z_A'.*

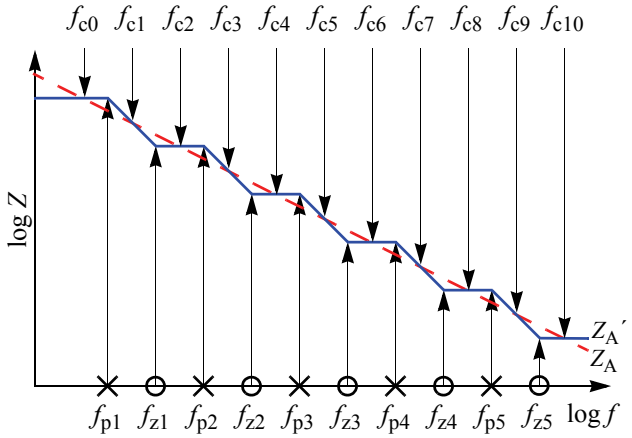

impedance of sC_0 for the overall model. Notice also that the frequencies at which the approximation Z_A' crosses Z_A are labeled and denoted f_{ci} on Figure 11.

Values for f_{ci} are found using

$$\log(f_{ci}) = \log(f_0) + i\left(\frac{\log(f_1) - \log(f_0)}{2N}\right), \tag{17}$$

$$f_{ci} = f_0\left(\frac{f_1}{f_0}\right)^{\frac{i}{2N}}, \tag{18}$$

where $f_0 = f_{c0}$ is the lowest frequency of interest, $f_1 = f_{c(2N-1)}$ is the highest frequency of interest, N is the order of the approximation network, and f_{ci} is the i^{th} crossing of Z_A' and Z_A.

From this information, the pole and zero frequencies are found to be

$$f_{pk} = -f_{c2k}\left(\frac{f_1}{f_0}\right)^{\frac{2k-\alpha}{2N}}, \tag{19}$$

$$f_{zk} = -f_{c2k}\left(\frac{f_1}{f_0}\right)^{\frac{2k+\alpha}{2N}}. \tag{20}$$

The above equations have been derived by applying simple geometric arguments to Figure 11. Partial fraction expansion is used to generate the residues of the poles [10],

$$Z_A'(0) = \left|Z_A(f_{c0})\right| = R_0, \tag{21}$$

$$Z_A'(s) = R_0 \prod_{k=1}^{N} \frac{\frac{s}{\omega_{zk}} - 1}{\frac{s}{\omega_{pk}} - 1}, \tag{22}$$

$$Z_A'(s) = A_\infty + \sum_{k=1}^{N} \frac{A_k}{\frac{s}{\omega_{pk}} - 1}, \tag{23}$$

where

$$A_\infty = R_0 \prod_{k=1}^{N} \frac{\omega_{pk}}{\omega_{zk}}, \tag{24}$$

$$A_k = Z_A'(s)\left(\frac{s}{\omega_{pk}} - 1\right)\Big|_{s=-\omega_{pk}}. \tag{25}$$

Each term in the partial fraction expansion is realized as a parallel RC pair,

$$Z(s) = \frac{R}{RCs + 1}, \tag{26}$$

$$R_k = A_k, \tag{27}$$

$$C_k = \frac{R}{\omega_{pk} R_k}. \tag{28}$$

The resulting circuit is shown in Figure 12. Alternatively, one could synthesize a parallel combination of series RC pairs by applying partial fraction expansion to $Y_A = 1/Z_A$.

FIGURE 12. *Model of capacitor of Figure 2.*

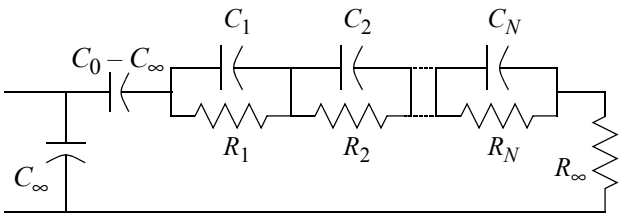

In Figure 13 the response of the model is compared against measured results. Z_A was approximated from 100 mHz to 10 MHz using 8 sections. An equivalent series resistance (ESR = 0.25 Ω) and inductance (ESL = 8 nH) have been added to model non-dielectric absorption related parasitics. The range of Z_A' was chosen so that it was accurate over all frequencies where it was significant. Thus it was accurately modeled down to the ESR corner frequency and up to the ESL resonant frequency. In Figures 14 through 16, the response of the model without ESR and ESL is compared to the results predicted by the Cole-Cole equation.

FIGURE 13. *Impedance of actual capacitor and model with 0.25 Ω ESR and 8 nH ESL.*

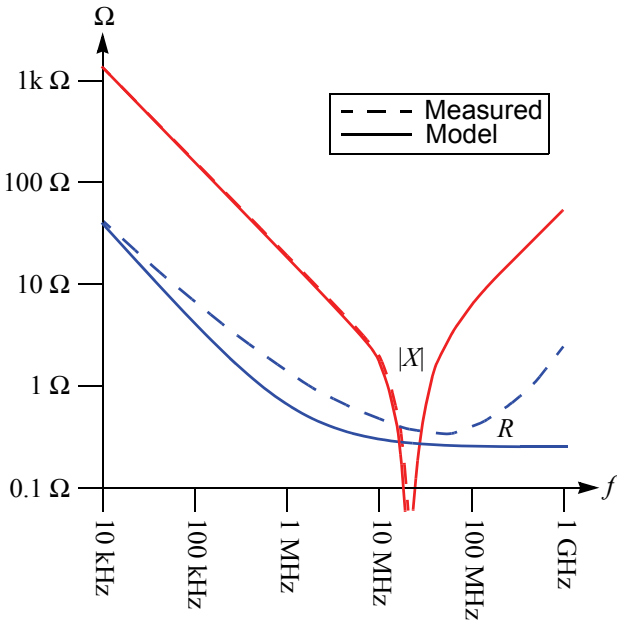

FIGURE 14. *Impedance of Cole-Cole relation (a) and model (b).*

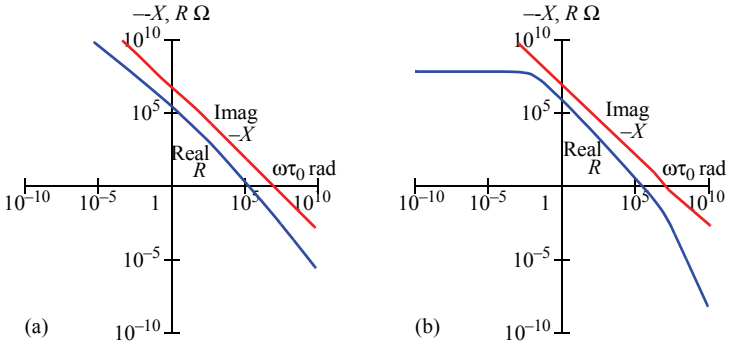

5.0 FracPole

A new type of basic element is being added to the Spectre circuit simulator that exhibits the following impedance,

$$Z(s) = As^{\beta}. \tag{29}$$

This new element is called a *fracpole*, which is short for fractional impedance pole. It approximates (29) over the range of frequencies from f_0 to f_1.

FIGURE 15. *Response of Cole-Cole relation (a) and model (b) to a negative current impulse.*

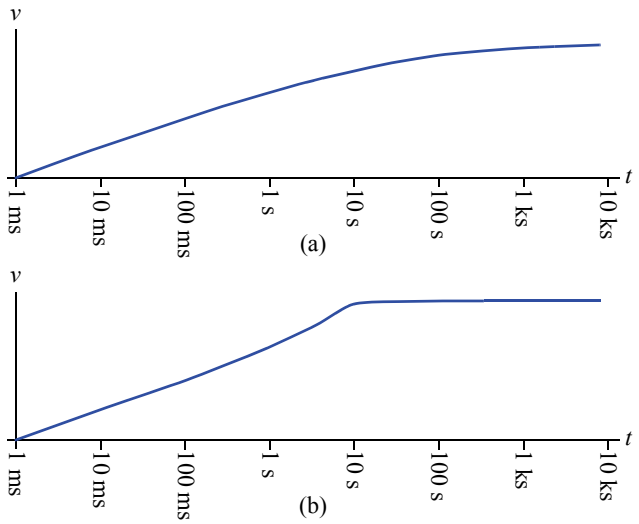

FIGURE 16. *Response of Cole-Cole relation (a) and model (b) to a positive voltage unit step.*

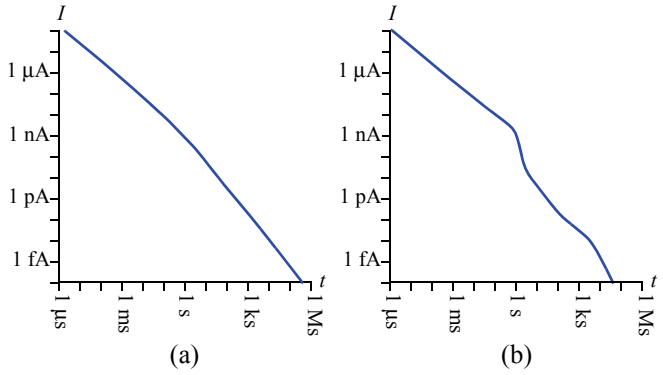

A subcircuit that implements the Cole-Cole capacitor model that uses the *fracpole* is shown in Figure 17 and an implementation is given in Listing 1

FIGURE 17. *Capacitor model that includes dielectric absorption.*

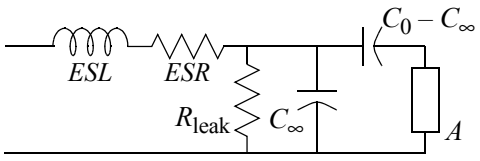

LISTING 1. *Capacitor model that includes dielectric absorption loss.*

```
simulator lang=spectre

subckt absorptivecap (1 2)
    parameters cinf c0 esr esl rleak tau0 alpha f0 f1
    L (1 3) inductor l=esl r=esr
    C (3 2) capacitor c=cinf
    Rl (3 2) resistor r=rleak
    Cx (3 4) capacitor c=c0–cinf
    DA (4 2) fracpole coef=pow(tau0,1–alpha)/(c0-cinf) slope=–alpha f0=f0 f1=f1 \
            profile=dd
ends absorptivecap
```

5.1 Interim Approach

Since the *fracpole* component is not yet available in Spectre, an alternative is available on an interim basis. A program, separate from Spectre, is available that takes the *fracpole* parameters and generates a Spectre subcircuit that implements it [17]. Also available is a program that takes a more direct approach. It takes the Cole-Cole parameters that describe the capacitor and uses the *fracpole* program to directly generate a Spectre subcircuit description of the form shown in Figure 17.

6.0 Conclusion

The importance of dielectric absorption at low frequencies is well known. It often limits the accuracy of analog sampled-data circuits such as sample-and-holds and switched-capacitor ADCs. However, as shown, dielectric absorption affects the behavior of the capacitor over its entire usable frequency range. As such, its affect at high frequencies, where it limits the *Q* of the capacitor, can be just as important, though it is generally not well understood or recognized.

Two models were given that are capable of accurately representing dielectric absorption over a very broad range of frequencies. These models allow designers to accurately determine the affect of dielectric absorption on their circuits.

6.1 If You Have Questions

If you have questions about what you have just read, feel free to post them on the *Forum* section of *The Designer's Guide Community* website. Do so by going to *www.designers-guide.org/Forum*.

Postscript

I would like to thank Robert Tso of TelASIC Communications, Inc. for pointing out several small errors in the manuscript and Cairong (or Charlie) Hu for pointing out a flaw in the *da* program.

Prof. J. A. Tenreiro Machado has pointed out that the fracpole is an application of fractional calculus (FC) modeling, and that there is a well established community studying FC and its applications. He continued by saying that the algorithm for modeling fractional poles with a collection of poles and zeros was first proposed by A. Oustaloup some years ago [19] and that Bohannan also published some interesting work where attempts to exploit the fractional order nature of capacitor, or what he calls 'fractance' [3], which is the characteristic exhibited by a 'fractor'. He references work that presents ideas similar to those presented in this paper, but based on a model of the dielectric developed by Curie that dates back to 1889 [15,24].

Fracpoles also play a role in modeling batteries [2], where a fracpole is referred to as a *Warburg element* and is used to model electrochemical diffusion. There are several diffusion models, but the simplest is the Warburg element [13]. A Warburg impedance element can be used to model semi-infinite linear diffusion, that is, unrestricted diffusion to a large planar electrode. Its impedance is

$$Z_W = \frac{A_W}{\sqrt{j\omega}}. \tag{30}$$

One models a parallel plate electrochemical cell using Randles' circuit, which employs a Warburg element to represent the electrochemical diffusion. Randles' circuit is an equivalent electrical circuit that consists of an active electrolyte resistance R_S in series with the parallel combination of the double-layer capacitance C_{dl} and the impedance of a faradaic reaction. The impedance of a faradaic reaction consists of an active charge transfer resistance R_{ct} and a specific electrochemical element of diffusion A_W, which is the Warburg element [1,22,25].

FIGURE 18. *Randles circuit model of an electrochemical cell.*

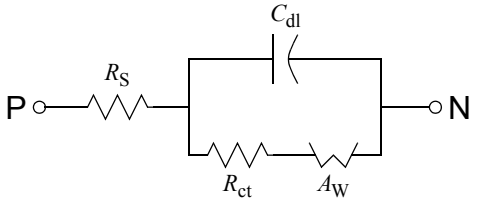

References

[1] Bard &. Faulkner. *Electrochemical Methods: Fundamentals and Applications*. Second Edition, 2000.

[2] Baudry, P. et al, Electro-thermal modelling of polymer lithium batteries for starting period and pulse power, *Journal of Power Sources*, vol 54, pp. 393-396, 1995.

[3] Gary W. Bohannan. *Analog Realization of a Fractional Control Element – Revisited*, October 27, 2002, Wavelength Electronics, Inc. Available on the web from *http://mechatronics.ece.usu.edu/foc/cdc02tw/cdrom/aditional/FOC_Proposal_Bohannan.pdf*.

[4] J. C. Burfoot and G. W. Taylor. *Polar Dielectrics and Their Applications*. University of California Press, Berkeley, 1979.

[5] R. Coelho. *Physics of Dielectrics for the Engineer*. Elsevier Scientific, New York, 1979.

[6] K. S. Cole and R. H. Cole. Dispersion and absorption in dielectrics — I. alternating current characteristics. *Journal of Chemical Physics*, vol. 9. Apr. 1941.

[7] K. S. Cole and R. H. Cole. Dispersion and absorption in dielectrics — II. direct current characteristics. *Journal of Chemical Physics*, vol. 10. Feb. 1942.

[8] R. H. Cole. Theories of dielectric polarization and relaxation. In *Progress in Dielectrics*, vol 3, Heywood 1961.

[9] P. DeBye. *Polar Molecules*. Chemical Catalog Co., New York, 1929.

[10] C. A. Desoer and E. S. Kuh. *Basic Circuit Theory.* McGraw-Hill, New York, 1969. TK454.2.D4.

[11] P. C. Dow. An analysis of certain errors in electronic differential analyzers — II. capacitor dielectric absorption. *IRE Transactions on Electrical Computers*, vol EC7, March 1958.

[12] J. W. Fattaruso, M. De Wit, G. Warwar, K.-S. Tan, and R. K. Hester. The effect of dielectric relaxation on charge-redistribution A/D converters. *IEEE Journal of Solid-State Circuits*, vol. 25, no. 6, Dec. 1990, pp. 1550-1561.

[13] Fitting EIS Data – Diffusion Elements – Warburg. *www.consultrsr.com/resources/eis/diffusion.htm.*

[14] C. Iorga. Compartmental analysis of dielectric absorption in capacitors. *IEEE Transactions on Dielectrics and Electrical Insulation*, vol. 7, no. 2, Apr. 2000, pp. 187-192.

[15] A. K. Jonscher. *Dielectric Relaxation in Solids*. Chelsea Dielectric Press, London, 1983.

[16] J. C. Kuenen and G. M. Meijer. Measurement of dielectric absorption of capacitors and analysis of its effects on VCOs. *IEEE Transactions on Instrumentation and Measurement*, vol. 45, no. 1, Feb. 1996, pp. 89-97.

[17] K. Kundert. *The FracPole Suite*. Available from *www.designers-guide.org/Modeling*. Includes executables and documentation.

[18] R. E. Lafferty. Capacitor loss at radio frequencies. *IEEE Transactions of Components, Hybrids, and Manufacturing Technology*, vol 15, no. 4, Aug. 1992.

[19] A. Oustaloup, La Commande CRONE: Commande Robuste d'Ordre Non Entier, Hermes, 1991.

[20] R. A. Pease. Understand capacitor soakage to optimize analog systems. *EDN*, 13 Oct. 1990, pp. 125-129. Can also be found at *www.national.com/rap*.

[21] S. Ramo, J. R. Whinnery and T. Van Duzer. *Fields and Waves in Communication Electronics*. John Wiley and Sons, New York, 1965.

[22] J.E. Randles. Kinetics of rapid electrode reactions. *Faraday Soc*. 1 (1947) 11.

[23] B. Seguin, J. P. Gosse, A. Sylvestre, A. P. Fouassier, and J. P. Ferrieux. Calorimetric apparatus for measurement of power losses in capacitors. *IEEE Instrumentation and Measurement Technology Conference*, May, 1998.

[24] S. Westerlund and L. Ekstam. Capacitor theory. *IEEE Transactions on Dielectrics and Electrical Insulation*, vol. 1, no. 5, pp. 826-839, October 1994.

[25] Wikipedia. Randles circuit. *en.wikipedia.org/wiki/Randles_circuit.*